

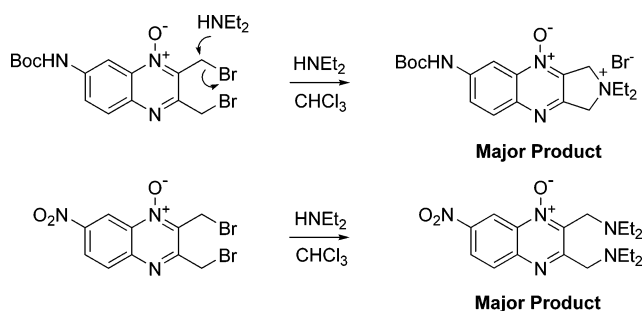
An Improved Understanding of the Reaction of Bis(bromomethyl)quinoxaline 1-*N*-Oxides with Amines Using Substituent Effects

Kathryn M. Evans, Alexandra M. Z. Slawin, Tomas Lebl, Douglas Philp, and Nicholas J. Westwood*

School of Chemistry and Centre of Biomolecular Sciences, University of St. Andrews, North Haugh, St. Andrews, KY16 9ST, United Kingdom

njw3@st-andrews.ac.uk; dp12@st-andrews.ac.uk

Received November 19, 2006



The reaction of bis(bromomethyl)quinoxaline *N*-oxides with amines is interesting from a reaction mechanism perspective and due to the reported biological activity of compounds in this general class. The complex mechanism of this reaction (particularly in the case of primary amines) is complicated further when C6 or C7 substituted mono-*N*-oxides are considered. In this study, the synthesis and subsequent characterization of a series of 2,3-bis(bromomethyl)quinoxaline 1-*N*-oxides is reported. Experimental and computational evidence is used to show that the observed product ratios from the reaction with diethylamine reflect the influence of both the C6/C7 substituent and the *N*-oxide functional group on the initial nucleophilic substitution reaction.

Introduction

Bis(bromomethyl)quinoxaline *N*-oxides are of interest due to their known biological activity and chemical reactivity. For example, di-*N*-oxides of general type **1** have been shown to possess antibacterial and antiparasitic activity.^{1,2} **2** has also been shown to exhibit a selective biological activity profile across a series of assays designed to probe host cell invasion by the parasite *Toxoplasma gondii*. On inspection this is a surprising result given that **2** appears to be a general alkylating agent. In our initial studies on this system,³ we considered the possibility that **2** exhibits this unexpected activity profile due to its mechanism of reaction with amines. We reported the first

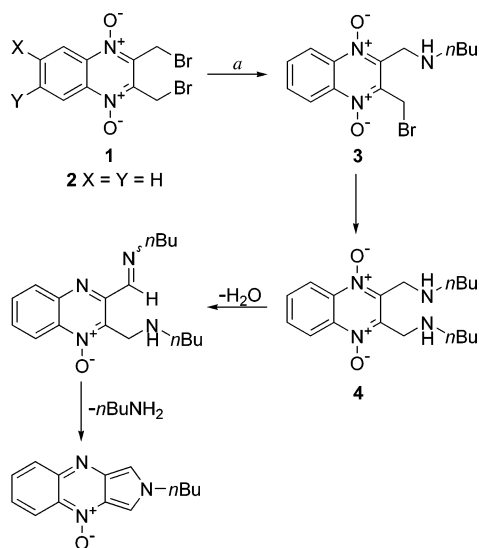
experimental evidence in support of a mechanism for this transformation (Scheme 1). In addition, an explanation of why **3** reacts to form the disubstituted intermediate **4** rather than undergoing a cyclization reaction was provided. We reasoned that electrostatic repulsion between the *N*-oxide oxygen and the departing bromine atom in **3** prevents access to the transition state required for an intramolecular S_N2 displacement. Computational studies played an important role in supporting this hypothesis.

These studies also led to an interesting prediction about the reaction of 2,3-bis(bromomethyl)quinoxaline 1-*N*-oxides (e.g., **5**) with amines (Scheme 2). In particular, we showed that reaction of **5** with diethylamine led to the formation of two products **6** and **7**, in a ratio of 63:37 respectively. This ratio has subsequently been shown by us to be relatively independent of the nature of the solvent suggesting that hydrogen bonding interactions between, for example, the oxygen of the *N*-oxide functional group and the incoming nucleophile do not significantly affect the outcome of this reaction (Scheme 2).⁴

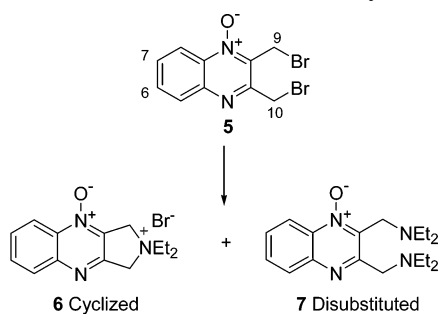
(1) Similar compounds have also been shown to exhibit antibacterial activity. McIlwain, H. *J. Chem. Soc.* **1943**, 322–325. Kim, H. K.; Miller, L. F.; Bambrury, R. E.; Ritter, H. W. *J. Med. Chem.* **1977**, *20*, 557–560.

(2) Carey, K. L.; Westwood, N. J.; Mitchison, T. J.; Ward, G. E. *Proc. Natl. Acad. Sci. U.S.A.* **2004**, *101*, 7434–7438.

(3) Pearson, R. J.; Evans, K. M.; Slawin, A. M. Z.; Philp, D.; Westwood, N. J. *J. Org. Chem.* **2005**, *70*, 5055–5061.

SCHEME 1. Reaction of 2 with an Excess of a Primary Amine, *n*-Butylamine^a

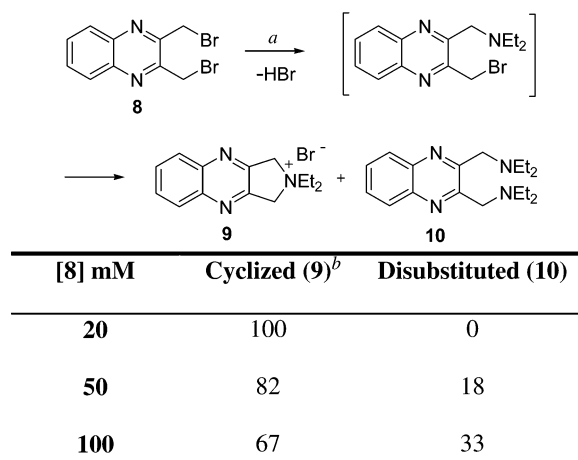
^a Reagents and conditions: (a) *n*-butylamine, CDCl₃, 25 °C.

SCHEME 2. Reaction of 5 with a Secondary Amine

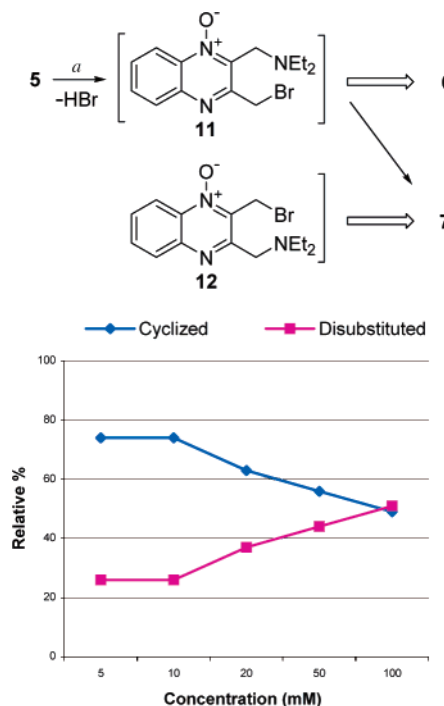
	Cyclized (6)	Disubstituted (7)
CDCl ₃	63 ^a	37 ^a
<i>d</i> ₆ -DMSO	60 ^b	40 ^b

^a From ref 3. ^b Average of 8 data points.

In attempting to rationalize the observed product ratio we made two assumptions: (1) initial displacement of the bromine atom adjacent to the *N*-oxide functional group in **5** (C9-Br) led exclusively to formation of the cyclized product **6** and (2) initial displacement of the alternative bromine atom (C10-Br) afforded the disubstituted product **7**.³ If correct, these two assumptions dictate that the observed product ratio directly reflects the ratio of the initial attack of the nucleophile at C9 and C10 in **5**. X-ray crystallographic analysis of **5** showed that the C9-Br bond was longer than the C10-Br bond supporting favored attack adjacent to the *N*-oxide, culminating in preferential formation of the cyclized product **6**. While this explanation was initially gratifying, we remained concerned about using a “ground state” observation such as X-ray structure determined bond length to rationalize the outcome of this reaction. In addition, a later observation regarding the concentration dependence of the

SCHEME 3. Reaction of 8 with a Secondary Amine^a

^a Reagents and conditions: (a) diethylamine (4 equiv), CDCl₃, 25 °C, 74% isolated yield of **9** (20 mM). ^b All values correspond to relative amounts of **9** and **10**.

SCHEME 4. Concentration Dependence of the Reaction of 5 with Diethylamine

^a Reagents and conditions: (a) diethylamine (4 equiv), CDCl₃, 25 °C.

reaction of 2,3-bis(bromomethyl)quinoxaline (**8**) with diethylamine refocused our interest in this work (Scheme 3). Here we provide a detailed study of the reaction of a series of 2,3-bis(bromomethyl)quinoxaline 1-*N*-oxides with diethylamine. Through the study of substituent effects on product ratios coupled with further computational studies we have gained a more detailed mechanistic understanding of this reaction.

Results and Discussion

Assessing the Validity of Assumptions 1 and 2. Previously our studies showed that when carried out at an initial concentra-

(4) Raposo, C.; Wilcox, C. S. *Tetrahedron Lett.* **1999**, *40*, 1285–1288.

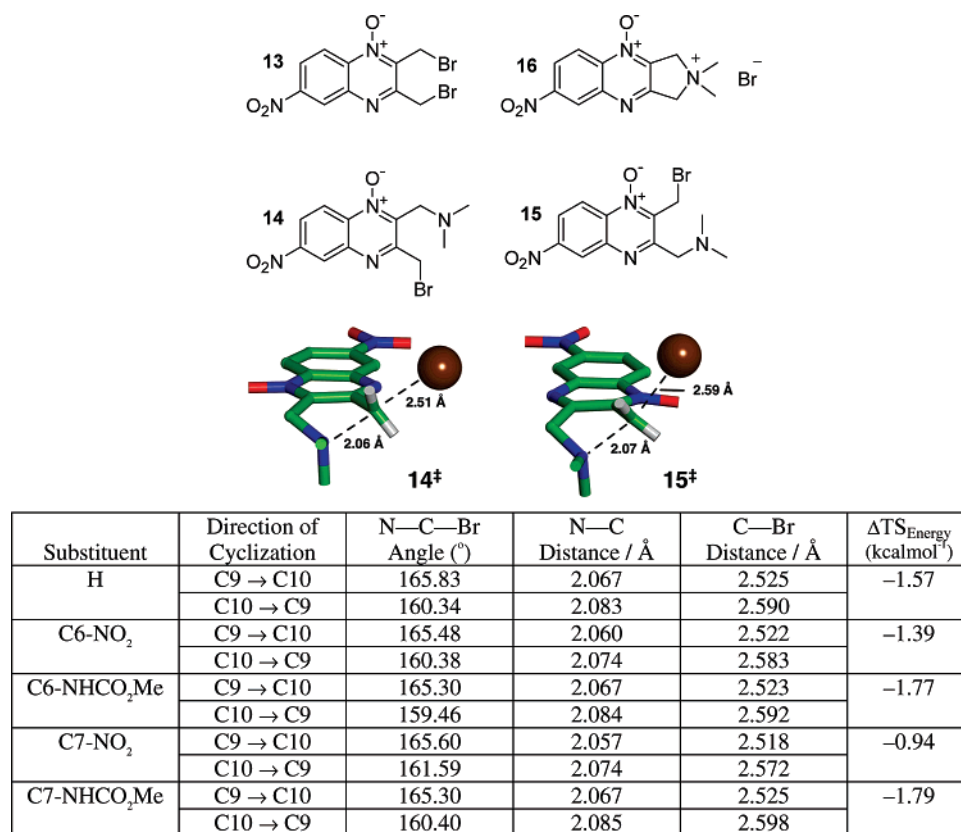


FIGURE 1. Calculated structures (B3LYP/6-31G(d,p)) of transition states 14^\ddagger and 15^\ddagger leading to cyclized product **16** from intermediates **14** and **15**, respectively. Transition state 14^\ddagger is more stable by 1.39 kcal mol⁻¹ at this level of theory. Carbon atoms are green, nitrogen atoms are blue, oxygen atoms are red, bromine atoms are brown, and hydrogen atoms are light gray. Most hydrogen atoms have been omitted for clarity.

tion of **8** of 20 mM in CDCl₃, **8** reacted with diethylamine to give **9** as the only observed product.³ When this reaction was repeated with increasing concentrations of **8** and diethylamine in the same proportions, a mixture of two products **9** and **10** was obtained consistent with effective intermolecular competition over the previously dominant cyclization reaction (Scheme 3). An analogous study with **5** showed a similar trend (Scheme 4) consistent with a view that our previous assumption 1 does not hold at higher reaction concentrations.

It was reasoned that information on the validity of assumption 2 could potentially be obtained by carrying out the reaction of **5** with diethylamine at lower concentrations. However, even at the lowest reaction concentrations that could be practically studied the ratio of **6**:**7** remained constant, consistent with there being no breakdown of assumption 2 even at low nucleophile concentrations. We therefore concluded that provided a suitable reaction concentration was selected, assumptions 1 and 2 both hold and the ratio of **6**:**7** reflects the ratio of initial nucleophilic attack at C9 and C10. The question remained, however, as to why preferential attack at C9 was observed for **5**.

Assumptions 1 and 2 Hold When Substituents Are Present at C6/C7. Studying the dependence of the reaction of analogs of **5** that are substituted at the C6/C7 position with diethylamine was identified as a useful method of gaining further insight into this potentially complex reaction. However, these studies were only considered useful if assumptions 1 and 2 hold for the modified substrates. It was therefore decided to assess computationally whether incorporation of C6/C7 substituents would have a dramatic effect on the relative stabilities of the key

transition states for the cyclization reactions in each case. The transition states required for cyclization were calculated at the B3LYP/6-31G(d,p) level of theory by using the PCM solvation model for CHCl₃ (Figure 1). The transition states for the cyclization reaction were located by generation of initial guesses with use of the linear synchronous transit (LST) method and refinement of these initial guesses at the HF/6-31G(d) level. These transition states were then used as initial guesses for refinement at the B3LYP/6-31G(d,p) level of theory. All transition states were demonstrated to possess a single imaginary vibration corresponding to the reaction coordinate. The results obtained are summarized in Figure 1. It is striking that the transition state structures are almost invariant with respect to the substituent present (or, indeed, absent) at the C6 or the C7 position. In all cases, cyclization from C9 to C10 involves a transition state that is less distorted (N—C—Br angles all around 166°) compared to those involving cyclization in the opposite direction from C10 to C9 (N—C—Br angles all around 161°). Examination of the view along the edge of the forming five-membered ring emphasizes the structural differences in these transition states (Figure 1). The distortion required to accommodate the electrostatic repulsion generated at the transition state between the negatively charged oxygen atom of the *N*-oxide and the departing bromide in a cyclization from C10 to C9 is clearly evident. This repulsion results in significant distortion of the five-membered ring in transition state 15^\ddagger . By contrast, the negatively charged oxygen atom of the *N*-oxide and the departing bromide are on opposite sides of the molecule in 14^\ddagger and the transition state has a much less distorted geometry. These

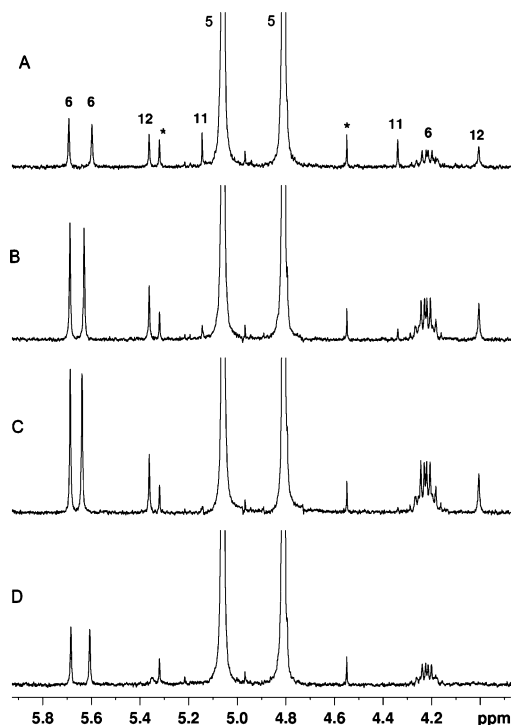


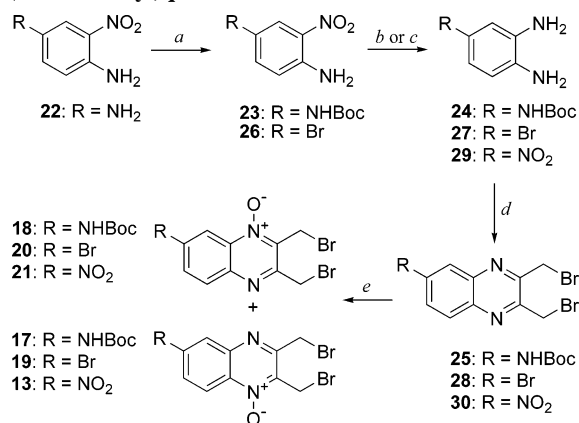
FIGURE 2. Reaction of **5** with limiting amounts of diethylamine in CDCl_3 monitored by ^1H NMR: (A) $t = 7$ min, (B) $t = 27$ min, (C) $t = 47$ min, and (D) $t = 360$ min. The asterisk indicates ^{13}C satellites of **5**.

observations mirror the behavior of the unsubstituted system **5** (see table in Figure 1) and our previous work³ on related systems.

The calculated energy difference ($\Delta\text{TS}_{\text{energy}}$) between the two cyclization transition states for each substituent (table in Figure 1) remains relatively constant as the substituent varies, supporting a view that the relative rates of the two cyclization reactions vary little with the substituent and hence the two assumptions hold across the series of compounds studied. A significant change in this calculated energy difference (and, hence, in the relative rate of cyclization) would be expected if, for example, one of the substituents dramatically facilitated the cyclization reaction following attack at C9.⁵ One possible explanation for the lack of a strong substituent effect on the relative rates of the cyclization reactions is the relatively poor overlap of the π -system of the quinoxaline 1-*N*-oxide with the σ^* orbital of the C–Br bond in the transition state for the cyclization reactions. *These computational studies therefore suggest that, provided the reactions of 5, 13, and 17–21 are carried out at a suitably low concentration, any observed dependence of product ratios on the substituent do not arise from the failure of assumptions 1 or 2.*

Observation of Reaction Intermediates. In an attempt to provide experimental evidence to support the above calculations, a ^1H NMR kinetic experiment was carried out on the reaction of **5** with a limiting quantity of diethylamine (1 equiv) in CDCl_3 at an initial concentration of **5** of 100 mM. This concentration was chosen to maximize the signal from any reaction intermediates. After 7 min post mixing three low-intensity sets of ^1H NMR signals were observed that were not present in the starting sample of **5**. These new signals were assigned to compounds

SCHEME 5. Synthesis of Substituted Bis(bromomethyl)quinoxaline 1-*N*-Oxides^a



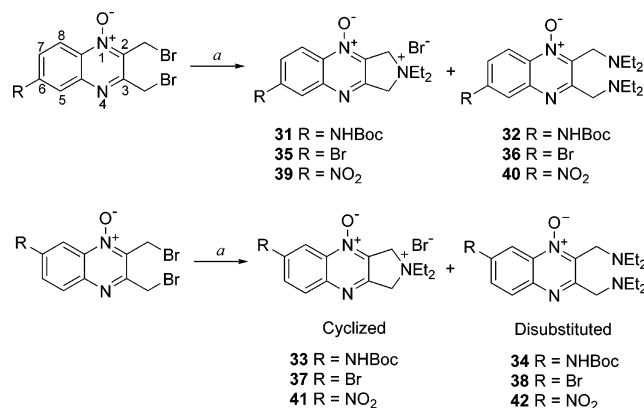
^a Reagents and conditions: (a) Boc anhydride, DCM, rt, 2 d, quant. **23**; (b) H_2 , 10% Pd/C, MeOH, rt, 24 h, 99% **24**; (c) $\text{SnCl}_2 \cdot 2\text{H}_2\text{O}$, EtOH, reflux, 93% **27**; (d) 1,4-dibromo-2,3-butanedione, THF, 0 °C to rt, 12–27 h, 88–95%; (e) *m*CPBA, DCM, rt/reflux, 24–48 h, 11–68%.

6, **11**, and **12** (Figure 2A, see the Supporting Information for a discussion of the NMR assignments).⁵ Interestingly, the signals corresponding to **11** had reduced significantly by 27 min (Figure 2B) and had disappeared within 47 min (Figure 2C) accompanied over this time period by an increase in the signals assigned to **6**. This observation is consistent with a view that **11** was converted relatively rapidly to **6** in line with the computational studies. In contrast, the size of the signals corresponding to intermediate **12** was relatively static over a much longer time period (Figure 2C). **12** only disappeared from the reaction after approximately 6 h (Figure 2D) presumably being converted to **6** as no signals corresponding to **7** were observed in this experiment. The kinetic data obtained in this experiment were used to estimate the relative rate of the two cyclization reactions (**11** or **12** to **6**) with use of the kinetic simulation package Gepasi.⁵ The calculations support a view that the conversion of **12** to **6** is at least an order of magnitude slower than the conversion of **11** to **6**.⁵ Signals corresponding to **11** and **12** were also observed when this experiment was repeated with **5** at an initial concentration of **5** of 10 mM (data not shown).

Interestingly, when the reaction of **13** with limiting quantities of diethylamine was analyzed at an initial concentration of **13** of 10 mM, signals corresponding to the formation of two intermediates were also observed (see the Supporting Information for ^1H NMR assignments). These intermediates behaved analogously to **11** and **12**, in that their relative stability with respect to cyclization mirrored that observed in experiments with **5**, again supporting the computational studies described above.⁵ Importantly, the fact that signals corresponding to intermediates in the reactions of both **5** and **13** were observed to grow in rapidly, plateau at low levels, and then decrease in intensity is consistent with the initial nucleophilic substitution reactions being rate-determining and hence important in determining the final product ratio. The low intensity of the ^1H NMR signals observed unfortunately made it very difficult to carry out a computational simulation that led to sufficiently accurate relative rates of the initial substitution reactions at C9 and C10 to be informative.

Observed Variation in the Product Ratio as a Function of the Substituent. Having shown through a series of compu-

(5) For further details see the Supporting Information.

TABLE 1. Product Distribution from Reaction of the Mono-N1-oxide 2,3-Bis(bromomethyl)quinoxaline Derivatives Bearing a C6/7 Substituent with Diethylamine^{a,b}

entry	compd	R	substituent position	C9–Br bond length (Å)	C10–Br bond length (Å)	cyclized ^c	disubstituted ^c
1	17	NHBoc	6	nd	nd	61 (31)	39 (32)
2	18	NHBoc	7	nd	nd	68 (33)	32 (34)
3	19	Br	6	1.979 (3) ^d	1.967(3)	55.5 (35)	44.5 (36)
4	20	Br	7	1.960 (18)	1.964 (15)	57 (37)	43 (38)
5	13	NO ₂	6	1.967 (3)	1.961 (3)	14 (39)	86 (40)
6	21	NO ₂	7	1.959 (3)	1.960 (3)	12.5 (41)	87.5 (42)

^a Reagents and conditions: (a) diethylamine (4 equiv), CDCl₃, 25 °C. ^b All values are an average of between 4 and 24 datapoints and errors are ±3 units. nd = not done. ^c Compound numbers shown in bold type. ^d Associated error shown in parentheses.

tational and ¹H NMR kinetic studies that incorporation of a substituent into **5** would not lead to a breakdown in assumptions 1 and 2, six analogues of **5** were prepared with substituents at the C6 and C7 positions.

Scheme 5 details how these analogues were prepared. With the exception of the NHBoc substituted analogues **17** and **18**, the remaining isomeric pairs were separable by column chromatography. Subsequent analysis of the reaction of **13** and **17–21** with diethylamine (4 equiv) was carried out in CDCl₃ at an

initial concentration of 20 mM. The results from these studies are shown in Table 1.

The data showed a clear difference in the product ratio as a function of the substituent, with the ratio of cyclized:disubstituted product decreasing as the electron-withdrawing nature of the substituent increased. This trend was mirrored in both the C6 and C7 series, with the results showing that there was little dependence of the product ratio on the position of the substituent (cf. entries 1 and 2).

Rationalization of the Observed Product Ratios. In our previous studies with **5**, the product ratio was rationalized based on the observed C9–Br and C10–Br bond lengths. However, this trend was not reproduced for **13**, **20**, and **21**, where the C9–Br and C10–Br bonds lengths determined from the crystal structures did not vary as expected given the observed product ratios (Table 1, entries 4–6). In addition, attempts to rationalize the observed ratios by using ¹³C NMR shifts as a readout of electron density at the C9 and C10 positions also failed.^{5–7}

Our favored explanation for the observed variation in chemical reactivity is best explained by initially considering the reaction of **17** and **18**, containing the electron-donating NHBoc substituent. As the computational studies and ¹H NMR support the view that assumptions 1 and 2 hold for **17** and **18**, the observed product ratio reflects the relative ratio of initial nucleophilic attack at the C9 and C10 positions. Given the known electronic influence of an NHBoc substituent, it would be expected that within the context of an S_N2 reaction, the transition states for the initial nucleophilic substitution reaction would be more S_N1-like with accumulation of positive charge

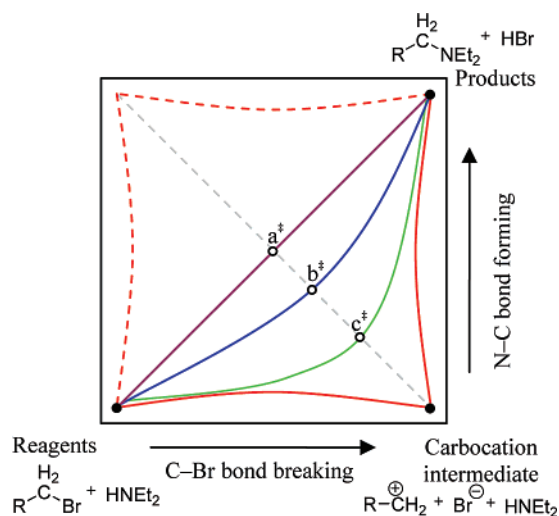
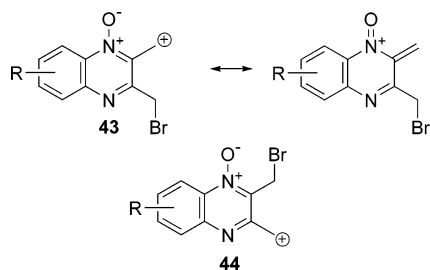


FIGURE 3. Schematic representation of a 2D energy surface illustrating the variation of the bond orders of the N–C and C–Br bonds in the reaction of a benzylic bromomethylene group with amines. The reaction coordinates are depicted for (i) the S_N1 process (red solid line), (ii) arbitrary reaction coordinates for the S_N2 process (purple, green, and blue lines), and (iii) the hypothetical limiting S_N2 process (red broken line). The transition states in the S_N2 reactions are labeled a⁺ (N–C ≈ C–Br), b⁺ (N–C < C–Br), and c⁺ (N–C ≪ C–Br). The image was adapted from refs 8 and 9.

(6) Cusack, K. P.; Arnold, L. D.; Barberis, C. E.; Chen, H.; Ericsson, A. M.; Gaza-Bulsecu, G. S.; Gordon, T. D.; Grinnell, C. M.; Harsch, A.; Pellegrini, M.; Tarcsa, E. *Bioorg. Med. Chem. Lett.* **2004**, *14*, 5503–5507.

(7) Spencer, S. R.; Xue, L. A.; Klenz, E. M.; Talalay, P. *Biochem. J.* **1991**, *273*, 711–717.

SCHEME 6. Structures 43 (with Resonance Form) and 44



at either C9 or C10 (i.e., transition state c^\ddagger , Figure 3).⁸ Comparison of the structures of the cations **43** (R = NHCO₂-Me) and **44** (R = NHCO₂Me) intuitively suggests a preference for the formation of a positive charge adjacent to the *N*-oxide functional group in **43** due to the increased resonance stabilization (Scheme 6). In line with the observed product ratio for **5**, it seems reasonable to propose that this is also the situation when no C6/C7 substituent is present, i.e., the preference for attack at C9 in **5** therefore results from the electronic influence of the *N*-oxide functional group on the reaction mechanism leading to most effective stabilization of developing positive charge at C9 and hence preferred initial nucleophilic substitution at this position leading to formation of **6** as the major product.

The question now becomes how can the observed change in the major product on incorporation of the strongly electron-withdrawing nitro functional group be rationalized (Table 1, entries 5 and 6). One likely explanation that builds on the arguments made above is that the perturbation caused by the nitro group on the initial substitution reaction leads to a reduction in the development of positive charge at the reactive centers compared with the NHBoc and H substrates (i.e., the reaction is more S_N2-like, transition state a^\ddagger , Figure 3). The influence of the *N*-oxide functional group on the reaction as depicted in Scheme 6 is essentially cancelled out and hence there is no dominant reaction observed through C9. The fact that the product resulting from C10 attack is the major product probably reflects another bias of this system either due to steric impediment to reaction at C9 compared with C10 or due to repulsion of the incoming nucleophile at C9 by the *N*-oxide oxygen, which does not occur at C10. In the case of the bromo-substituted series (Table 1, entries 3 and 4), the electron-withdrawing nature of the bromine substituent again modulates the influence of the *N*-oxide functional group resulting in a situation where the observed product ratios are consistent with less deviation from an idealized S_N2 transition state toward an S_N1-mechanism as compared with **5**. In all cases, one possible explanation for the insensitivity of the product ratio to the position of the substituent is the relatively remote nature of the substituent from the reaction center compared with, for example, analogous reactions of benzyl halides.⁸

Conclusion

Bis(bromomethyl)quinoxaline 1-*N*-oxides containing a substituent at either the C6 or C7 position have been synthesized and their reactivity with diethylamine assessed. While in all cases two products were formed, the ratio of the two products varied significantly depending on the electron-donating or

-withdrawing nature of the substituent. However, the position (C6 or C7) of the substituent had only subtle effects on the reaction outcome. A combination of experimental and computational analysis supports the view that, under the reaction conditions used, the product ratio mirrored the relative propensity of diethylamine to attack at C9 or C10 in the initial nucleophilic substitution reaction. Rationalization of the results by using ground state analysis of the reactants (X-ray crystallography, ¹³C NMR) was not possible. However, the observed variation in the product ratios as a function of the substituent can be explained by considering the deviation from an ideal S_N2 reaction induced by the substituents and the ability of the *N*-oxide functional group to stabilize positive charge that develops at C9 in the transition state. These studies have provided a detailed understanding of the mechanism of this interesting chemical reaction and enabled us to provide an improved explanation of the observed product ratio obtained on reaction of **5** with diethylamine. Furthermore, these studies will contribute to our attempts to explain the mode of action of compounds of this general class.¹⁻³

Experimental Section

General Methods. Unless otherwise noted, starting materials and reagents were obtained from commercial suppliers and were used without further purification. Dichloromethane (DCM) was dried by heating under reflux over calcium hydride and distilled under an atmosphere of nitrogen. mCPBA was purified by dissolving in DCM and washing with an aqueous solution of buffered KH₂PO₄ (1.0 M) at pH 7.4–7.5. The DCM phase was then treated as for a separation. PE 40–60 refers to the fraction of light PE 40–60 boiling in the range of 40–60 °C. Melting points were recorded on an Electrothermal 9100 capillary melting point apparatus. Values are quoted to the nearest 0.5 °C. IR spectra were measured on a Perkin-Elmer Paragon 1000 FT-IR spectrometer. ¹H NMR spectra were recorded at 300 and 500 MHz. ¹³C NMR spectra were recorded at either 75 or 125 MHz. *J* values are quoted in Hz. Low- and high-resolution mass spectral analyses were recorded in either EI, CI, or ES operating in positive ion mode.

***tert*-Butyl 4-Amino-3-nitrophenylcarbamate (23).** **23** was prepared by a procedure reported by Smith et al.¹⁰ Di-*tert*-butyldicarbonate (48.0 g, 0.22 mol) was added to a solution of 2-nitro-*p*-phenylenediamine (30.6 g, 0.20 mol) in anhydrous DCM (1.00 L) at room temperature, under nitrogen. After being stirred for 2 d the reaction mixture was diluted with DCM (1.00 L) and washed with 10% w/v aqueous NaHCO₃ solution (2 × 500 mL). The organic phase was washed with brine (500 mL) and the combined aqueous phases extracted with DCM (2 × 500 mL). The combined organic phases were dried (MgSO₄) and concentrated in vacuo. Drying under vacuum at 50 °C gave **23** as a bright orange solid (50.7 g, 0.20 mol, quant.); mp 135.0–137.0 °C. IR (NaCl, Nujol) ν_{max} : 3500, 3381, 3335, 1691, 1531, 1252, 1218, 1161, 887, 822, 747 cm⁻¹. ¹H NMR (300 MHz, DMSO-*d*₆): δ 9.28 (br s, 1H), 8.20 (br s, 1H), 7.40 (dd, ³*J* = 9.1 Hz, ⁴*J* = 2.5 Hz, 1H), 7.25 (s, 2H), 6.95 (d, ³*J* = 9.1 Hz, 1H), 1.46 (s, 9H). ¹³C NMR (75.5 MHz, DMSO-*d*₆): δ 152.8 (C), 142.3 (C), 129.3 (C), 128.5 (CH), 128.2 (C), 119.4 (CH), 112.6 (CH), 79.0 (C), 28.0 (3 × CH₃). MS-EI+ (*m/z*) 253 ([M]⁺, 4%), 197 (45), 153 (25). HRMS-EI+ (*m/z*) calcd for C₁₁H₁₅N₃O₄ [M]⁺ 253.1063, found 253.1063. Anal. Calcd for C₁₁H₁₅N₃O₄: C, 52.17; H, 5.97; N, 16.59. Found: C, 52.39; H, 6.07; N, 16.35.

***tert*-Butyl 3,4-Diaminophenylcarbamate (24).** A 250 mL round-bottomed flask equipped with **23** (4.00 g, 15.8 mmol) and 10% Pd/C (0.80 g) was purged with nitrogen. MeOH (60.0 mL) was

(8) Shpan'ko, I. V.; Korostylev, A. P.; Rusu, L. N. *J. Org. Chem. USSR (Transl.)* **1984**, *20*, 1881–1888.

(9) Scudder, P. H. *Electron Flow in Organic Chemistry*; John Wiley & Sons, Inc.: New York, 1992.

(10) Smith, D. M.; McFarlane, M. D.; Moody, D. J. *J. Chem. Soc., Perkin Trans. I* **1988**, 691–696 and references cited therein.

added with stirring and the flask covered in foil. The flask was then purged with hydrogen and a hydrogen balloon introduced that was replaced a further 3 times. After 24 h of stirring at room temperature the reaction mixture was filtered over Celite washing with MeOH (300 mL). Removal of the solvent in vacuo afforded the desired product **24** as an off-white crystalline solid (3.50 g, 15.7 mmol, 99%) that was used without any further purification. IR (NaCl, Nujol) ν_{max} : 3410–3215, 1725, 1700, 1610, 1521, 1243, 1166, 1059, 850, 810–720 cm^{-1} . ^1H NMR (300 MHz, CDCl_3): δ 6.92 (br s, 1H), 6.59 (d, $^3J = 8.2$ Hz, 1H), 6.50 (dd, $^3J = 8.2$ Hz, $^4J = 2.3$ Hz, 1H), 6.37 (br s, 1H), 3.23 (br s, 4H), 1.49 (s, 9H). ^{13}C NMR (75.5 MHz, CDCl_3): δ 153.1 (C), 135.7 (C), 131.5 (C), 129.9 (C), 117.2 (CH), 110.5 (CH), 108.0 (CH), 80.0 (C), 28.3 (3 \times CH_3).

General Procedure for the Preparation of the C6-Substituted 2,3-Bis(bromomethyl)quinoxalines: 2,3-Bis(bromomethyl)-6-bromoquinoxaline (28). A solution of 1,4-dibromo-2,3-butanedione (529 mg, 2.17 mmol) in anhydrous THF (20 mL) was added dropwise to a solution of **27**¹¹ (398 mg, 2.13 mmol) in anhydrous THF (20 mL) at 0 °C over 15 min with stirring. The reaction was warmed to room temperature and stirred for a further 27 h. After concentration in vacuo, the crude material was redissolved in DCM (100 mL) and partitioned between 10% w/v aqueous NaHCO_3 solution (200 mL) and DCM (300 mL). The organic phase was washed with brine (100 mL), dried (MgSO_4), filtered, and concentrated in vacuo to give a pale brown solid. Purification by flash column chromatography on silica gel (EtOAc:PE 40–60, 1:9) gave **28** as a white crystalline solid (736 mg, 1.86 mmol, 88%); mp 143.0–144.0 °C. IR (KBr) ν_{max} : 3090, 3027, 2968, 1597, 1476, 1419, 1357, 1211, 939, 833, 799, 722, 638, 603, 569, 426 cm^{-1} . ^1H NMR (300 MHz, CDCl_3): δ 8.24 (d, $^4J = 2.1$ Hz, 1H), 7.92 (d, $^3J = 8.9$ Hz, 1H), 7.85 (dd, $^3J = 8.9$ Hz, $^4J = 2.1$ Hz, 1H), 4.89 (s, 4H). ^{13}C NMR (75 MHz, CDCl_3): δ 151.8 (C), 151.1 (C), 142.0 (C), 140.2 (C), 134.4 (CH), 131.3 (CH), 130.2 (CH), 125.1 (C), 30.2 (CH_2), 30.1 (CH_2); MS-ES+ (m/z) 399 ([M + H]⁺, 3 \times ^{81}Br , 23%), 397 ([M + H]⁺, 2 \times ^{81}Br + ^{79}Br , 95), 395 ([M + H]⁺, 2 \times ^{79}Br + ^{81}Br , 100), 393 ([M + H]⁺, 3 \times ^{79}Br , 25). Anal. Calcd for $\text{C}_{10}\text{H}_7\text{Br}_3\text{N}_2$: C, 30.42; H, 1.79; N, 7.09. Found: C, 30.50; H, 1.60; N, 6.94.

General Procedure for the Oxidation of 2,3-Bis(bromomethyl)quinoxalines: 2,3-Bis(bromomethyl)-6-bromoquinoxaline 1-Oxide (19). To a solution of **28** (312 g, 0.79 mmol) in anhydrous DCM (20.0 mL) was added purified *m*CPBA (1.02 g, 5.93 mmol) with stirring. After 34 h at room temperature the reaction mixture was diluted with DCM (20.0 mL) and washed with 10% w/v Na_2CO_3 solution (3 \times 20 mL). The organic phase was dried (MgSO_4), filtered, and concentrated in vacuo to give a yellow solid. Purification by flash column chromatography on silica gel (EtOAc:PE 40–60, 1:19 to 1:9) gave **19** as a pale yellow solid (37 mg, 0.09 mmol, 18%); mp 144.5–146.0 °C. IR (NaCl, Nujol) ν_{max} : 3450, 1595, 1567, 1351, 1204, 1168, 1107, 1057, 823, 774, 683, 670 cm^{-1} . ^1H NMR (300 MHz, $\text{DMSO}-d_6$): δ 8.40 (d, $^4J = 2.1$ Hz, 1H), 8.36 (d, $^3J = 9.2$ Hz, 1H), 8.02 (dd, $^3J = 9.2$ Hz, $^4J = 2.1$ Hz, 1H), 5.00 (s, 2H), 4.99 (s, 2H). ^1H NMR (300 MHz, CDCl_3): δ 8.39 (d, $^3J = 9.2$ Hz, 1H), 8.23 (d, $^4J = 2.0$ Hz, 1H), 7.80 (dd, $^3J = 9.2$ Hz, $^4J = 2.0$ Hz, 1H), 4.96 (s, 2H), 4.73 (s, 2H). ^{13}C NMR (75.5 MHz, CDCl_3): δ 153.8 (C), 143.9 (C), 138.8 (C), 135.3 (C), 134.2 (CH), 132.2 (CH), 126.8 (C), 120.7 (CH), 29.9 (CH_2), 20.6 (CH_2). MS-ES+ (m/z) 435 ([M + Na]⁺, 2 \times ^{81}Br + ^{79}Br , 79), 433 ([M + Na]⁺, 2 \times ^{79}Br + ^{81}Br , 100). HRMS-ES+ (m/z) calcd for $\text{C}_{10}\text{H}_7^{79}\text{Br}^{81}\text{Br}_2\text{N}_2\text{O}_2\text{Na}$ [M + Na]⁺ 434.7965, found 434.7953. HRMS-ES+ (m/z) calcd for $\text{C}_{10}\text{H}_7^{79}\text{Br}_2^{81}\text{BrN}_2\text{O}_2\text{Na}$ [M + Na]⁺ 432.7986, found 432.7975. The structure was also confirmed by X-ray crystallographic analysis.⁵ **2,3-Bis(bromomethyl)-7-bromoquinoxaline 1-Oxide (20).** **20** was also collected as a white crystalline solid (30 mg, 0.07 mmol, 14%); mp

> 180 °C dec. IR (NaCl, Nujol) ν_{max} : 3450, 1597, 1561, 1355, 830, 774, 672 cm^{-1} . ^1H NMR (300 MHz, CDCl_3): δ 8.73 (br d, $^4J = 1.8$ Hz, 1H), 7.92 (m, 2H), 4.98 (s, 2H), 4.74 (s, 2H). ^{13}C NMR (75.5 MHz, CDCl_3): δ 152.9 (C), 142.1 (C), 139.1 (C), 136.7 (C), 135.9 (CH), 131.4 (CH), 125.6 (C), 122.0 (CH), 30.0 (CH_2), 20.5 (CH_2). MS-ES+ (m/z) 435 ([M + Na]⁺, 2 \times ^{81}Br + ^{79}Br , 74), 433 ([M + Na]⁺, 2 \times ^{79}Br + ^{81}Br , 100). HRMS-ES+ (m/z) calcd for $\text{C}_{10}\text{H}_7^{79}\text{Br}^{81}\text{Br}_2\text{N}_2\text{O}_2\text{Na}$ [M + Na]⁺ 434.7965, found 434.7955. HRMS-ES+ (m/z) calcd for $\text{C}_{10}\text{H}_7^{79}\text{Br}_2^{81}\text{BrN}_2\text{O}_2\text{Na}$ [M + Na]⁺ 432.7986, found 432.7980. Anal. Calcd for $\text{C}_{10}\text{H}_7\text{Br}_3\text{N}_2\text{O}_2$: C, 29.23; H, 1.72; N, 6.82. Found: C, 29.49; H, 1.43; N, 6.60. The structure was also confirmed by X-ray crystallographic analysis.⁵ **2,3-Bis(bromomethyl)-6-bromoquinoxaline 1,4-dioxide**¹² was also collected as a bright yellow crystalline solid (184 mg, 0.43 mmol, 55%).

General Procedure for Reactions of 2,3-Bis(bromomethyl)quinoxalines with Diethylamine. To a solution of the quinoxaline derivative (0.5 mL of a 40 mM solution in CDCl_3) was added a solution of diethylamine (0.5 mL of a 120 mM solution in CDCl_3) in an NMR tube at 25 °C and the mixture was then monitored by 300 MHz ^1H NMR. The excess of diethylamine was used to drive the reactions to completion, in order to assist interpretation of the ^1H NMR spectra.

2,2-Diethyl-2,3-dihydro-1H-pyrrolo[3,4-*b*]-7-bromoquinoxalin-2-ium Bromide 4-Oxide (35). **35** was prepared according to the general procedure with **19** and diethylamine. Reaction was scaled up 6-fold for full analysis. **35** was collected following crystallization to yield a white crystalline solid (16 mg, 0.04 mmol, 35%); mp > 195 °C dec. IR (NaCl, Nujol) ν_{max} : 3458, 1597, 1571, 1368, 1107, 820, 743, 723 cm^{-1} . ^1H NMR (300 MHz, $\text{DMSO}-d_6$): δ 8.49 (d, $^4J = 2.1$ Hz, 1H), 8.42 (d, $^3J = 9.2$ Hz, 1H), 8.06 (dd, $^3J = 9.2$ Hz, $^4J = 2.1$ Hz, 1H), 5.26 (s, 2H), 5.23 (s, 2H), 3.72 (q, $^3J = 7.1$ Hz, 4H), 1.31 (t, $^3J = 7.1$ Hz, 6H). ^{13}C NMR (75.5 MHz, $\text{DMSO}-d_6$): δ 153.8 (C), 146.1 (C), 135.5 (C), 133.4 (C), 133.4 (CH) 131.6 (CH), 125.6 (C), 119.7 (CH), 65.4 (CH_2), 62.0 (CH_2), 57.7 (2 \times CH_2), 8.4 (2 \times CH_3); MS-ES+ (m/z) 324 ([M – Br]⁺, ^{81}Br , 87%), 322 ([M – Br]⁺, ^{79}Br , 100). HRMS-ES+ (m/z) calcd for $\text{C}_{14}\text{H}_{18}^{81}\text{BrN}_3\text{O}$ [M – Br]⁺ 324.0535, found 324.0538. HRMS-ES+ (m/z) calcd for $\text{C}_{14}\text{H}_{18}^{79}\text{BrN}_3\text{O}$ [M – Br]⁺ 322.0555, found 322.0552.

(3-(Diethylaminomethyl)-6-bromoquinoxalin-2-ylmethyl)diethylamine 1-Oxide (36). **36** was recovered from the filtrate in the presence of diethylamine. ^1H NMR (300 MHz, $\text{DMSO}-d_6$): δ 8.36 (d, $^3J = 9.2$ Hz, 1H), 8.32 (d, $^4J = 2.1$ Hz, 1H), 7.94 (dd, $^3J = 9.2$ Hz, $^4J = 2.1$ Hz, 1H), 4.24 (s, 2H), 4.06 (s, 2H), 2.63–2.49 (m, 8H), 0.95 (t, 12H). ^1H NMR (300 MHz, CDCl_3): δ 8.40 (d, $^3J = 9.2$ Hz, 1H), 8.23 (d, $^4J = 2.1$ Hz, 1H), 7.72 (dd, $^3J = 9.2$ Hz, $^4J = 2.1$ Hz, 1H), 4.28 (s, 2H), 4.10 (s, 2H), 2.65–2.54 (m, 8H), 1.02–0.97 (m, 12H). ^{13}C NMR (75.5 MHz, CDCl_3): δ 158.9 (C), 143.6 (C), 141.7 (C), 134.7 (C), 132.7 (CH), 131.9 (CH), 125.0 (C), 121.0 (CH), 57.6 (CH_2), 47.2 (CH_2), 47.0 (2 \times CH_2), 46.5 (2 \times CH_2), 11.3 (2 \times CH_3), 11.0 (2 \times CH_3). MS-ES+ (m/z) 397 ([M + H]⁺, ^{81}Br , 79%), 395 ([M + H]⁺, ^{79}Br , 100), 379 ([M – OH]⁺, ^{81}Br , 54), 395 ([M – OH]⁺, ^{79}Br , 55), 324 ([M – NEt_2]⁺, ^{81}Br , 28), 322 ([M – NEt_2]⁺, ^{79}Br , 32), 308 ([M – O – NEt_2]⁺, ^{81}Br , 56), 306 ([M – O – NEt_2]⁺, ^{79}Br , 83). HRMS-ES+ (m/z) calcd for $\text{C}_{18}\text{H}_{27}^{81}\text{BrN}_4\text{O}_2\text{Na}$ [M + Na]⁺ 419.1245, found 419.1262. HRMS-ES+ (m/z) calcd for $\text{C}_{18}\text{H}_{27}^{79}\text{BrN}_4\text{O}_2\text{Na}$ [M + Na]⁺ 417.1266, found 417.1264.

Acknowledgment. We acknowledge the input of an excellent reviewer who's suggestion it was to carry out the experiments using limiting concentrations of diethylamine that are described above and provided strong experimental evidence to support the computational work. We would like to acknowledge the assistance of Mrs. M. Smith for NMR, Mrs. C. Horsburgh

(11) Rangarajan, M.; Kim, J. S.; Sim, S-P.; Liu, A.; Liu, L. F.; La Voie, E. J. *Bioorg. Med. Chem.* **2000**, *8*, 2591–2600.

(12) Musatova, I. S.; Elina, A. S.; Solov'eva, N. P.; Polukhina, L. M.; Moskalenko, N. Y.; Pershin, G. N. *Pharm. Chem. J.* **1983**, *17*, 779–784.

for HRMS analysis, and Mrs. S. Williamson for elemental analysis. Financial support from BBSRC (No. 02/A1/B/08395 (KME), NIH (No. R01A1054961), and the Royal Society (NJW fellowship) is gratefully acknowledged.

Supporting Information Available: General experimental procedures and spectral data for previously unreported starting

materials and products, including ^1H and ^{13}C NMR spectra for the reaction of **17/18** with diethylamine, and Cartesian coordinates and total energies for the optimized structures of the calculated transition states. This material is available free of charge via the Internet at <http://pubs.acs.org>.

JO062380Y